

Design, synthesis, and antifungal activities in vitro of novel tetrahydroisoquinoline compounds based on the structure of lanosterol 14 α -demethylase (CYP51) of fungi

Ju Zhu, Jiaguo Lu, Youjun Zhou,* Yaowu Li, Jun Cheng and Canhui Zheng

Department of Medicinal Chemistry, School of Pharmacy, Second Military Medical University, Shanghai 200433, China

Received 27 February 2006; revised 16 July 2006; accepted 1 August 2006

Available online 14 August 2006

Abstract—Novel tetrahydroisoquinoline compounds were designed by coupling structure-based de novo design based on the structure of lanosterol 14 α -demethylase (CYP51). The chemical synthesis and the antifungal activities in vitro of them were reported. The results exhibited that all of the lead compounds showed potent antifungal activities, in which compounds **6** and **7** had equal or stronger antifungal activities against five test fungi than that of fluconazole. The studies presented here provided the antifungal lead compounds. The affinity of the lead molecules for CYP51 was mainly attributed to their non-bonding interaction with the apoprotein, which was different from the azole antifungal agents.

© 2006 Elsevier Ltd. All rights reserved.

Lanosterol 14 α -demethylase (CYP51) is one of the key enzymes of sterol biosynthesis in fungi¹ and is a prime target for development of antifungal drugs. The development of inhibitors of lanosterol 14 α -demethylase in fungi has provided azole antifungal drugs used in clinical therapy, such as ketoconazole, fluconazole, voriconazole, and itraconazole (Fig. 1).² These azole antifungal drugs are classified as imidazoles and triazoles on the basis of whether they have two or three nitrogens in the five-membered azole ring. Azole antifungal agents inhibit the CYP51 by a mechanism in which the heterocyclic nitrogen atom (N-3 of imidazole and N-4 of triazole) binds to the heme iron atom in the binding site of the enzyme. The resulting ergosterol depletion and the accumulation of precursor 14 α -methylated sterols interfere with the function of ergosterol as a membrane component. They disrupt the structure of the plasma membrane, making it more vulnerable to further damage, and alter the activities of several membrane-bound enzymes.^{3,4}

Because CYP51 is a member of the cytochrome P450 superfamily which exists in fungi and mammals, azole

antifungal agents are generally toxic and are hampered in the treatment of deep-seated mycoses and life-threatening systemic infections because of their ability to coordinate with the heme of a lot of host cytochrome P450 enzymes, particularly mammalian CYP3A4.^{5,6} Cases of fatal hepatotoxicity have been reported.^{7–12} The azole ring has been demonstrated to be one of the most important pharmacophores for antifungal activity, and both toxicity and activity of azole antifungal agents are mainly attributed to the coordination binding of the nitrogen atom of the azole ring to the iron atom of heme.^{13,14} All of these findings urged us to discover novel non-azole lead compounds with more structural specificity for the fungal enzyme to separate their activity from toxicity.

Because the crystal structure of CYP51 of fungi has not been obtained, in previous studies, we constructed a three-dimensional model of CYP51 from *Candida albicans*¹⁵ and investigated the active site of CYP51, then, we designed non-azole antifungal lead compounds based on the constructed three-dimensional model of CYP51 by coupling structure-based de novo design. The non-azole lead molecules containing benzopyran ring were successfully designed and synthesized. The results of their biological evaluation showed that the benzopyran compounds are the novel non-azole inhibitors specific for CYP51 of fungi.¹⁶ Although the antifungal activities of the designed lead compounds are much lower, these

Keywords: CYP51 inhibitor; Antifungal activity; Tetrahydroisoquinoline; Design; Lanosterol 14 α -demethylase (CYP51).

*Corresponding author. Tel.: +86 021 25070383; e-mail: zhouyoujun2006@yahoo.com.cn

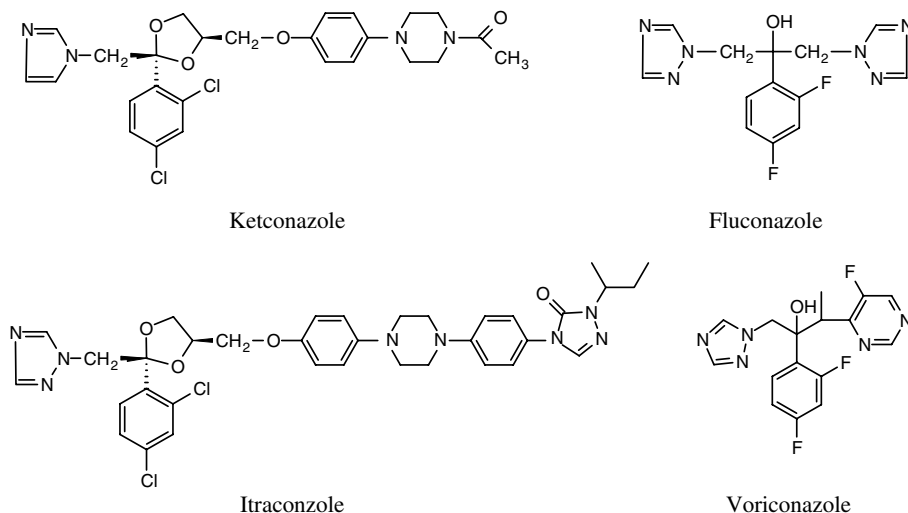


Figure 1. Azole antifungal drugs used in clinical therapy.

findings encouraged us to make further efforts to explore more potent non-azole antifungal lead compounds specific for fungi.

In this paper, the non-azole lead molecules were further designed according to the previous method,¹⁶ and the antifungal activity in vitro of the lead compounds was evaluated.

In previous study, we found that except for the site coordinating with the heme, the key regions in the active site of CYP51 for ligand non-covalent binding can be divided into four subsites by the investigation of the three-dimensional molecular model of CYP51 from *C. albicans*^{15,16}: S1–S4. The S1 subsite was the hydrophilic hydrogen-bonding region; the S2 subsite was the hydrophobic region; the S3 subsite was the narrow hydrophobic cleft formed by the residues in the helix B'-meander1 loop and the N terminus of helix I; The S4 subsite adjacent to the β 6-1/ β 1-4 sheet is another important hydrogen-bonding region in the active site.

Because the toxicity of azole antifungal agents is mainly attributed to the coordination binding of the nitrogen atom of the azole ring to the iron atom of heme, during the process of inhibitor design in the present study, only those functional groups forming non-covalent bonds with the amino acid residues in the active site of CYP51 were introduced, avoiding the connection with the iron atom of heme. By connecting the highest scoring minimum in each subsite, the lead structures were designed.

The lead molecules were constructed by manually linking some of the MCSS minima.¹⁷ The new bond was constructed in such a way that there was no introduction of significant internal strain in the candidate ligand. During the fragment connection step, the synthetic accessibility of the generated structures was taken into account. The newly formed ligand molecules were subsequently energy-minimized in the rigid protein to regularize the internal coordinates using the CVFF force field in the Discover 95.0 program within Insight II. The Affinity module within Insight II was then applied to define the lowest energy position for the generated molecules by using a Monte Carlo and simulated annealing combined protocol. All of the atoms within a defined radius (5 Å) of the lead molecules were allowed to move. The solvation grid supplied with the Affinity program was used.¹⁸ The resulting structure was accepted if it passed the Metropolis criterion and then a check of the rms distance of the new structure versus the structure found so far. The final conformations were obtained through a simulation annealing procedure from 500 to 300 K, and then 2000 rounds of energy minimization were performed to reach a convergence, where the resulting interaction energy values were used to define a rank order. Each energy-minimized final docking position of the lead molecules was evaluated using the interaction score function in the LUDI module.^{19,20}

Figure 2 shows some of the designed lead molecules containing the tetrahydroisoquinoline ring.

At position 2 of the lead structure, long lipophilic alkyl side chains were introduced to interact with the hydro-

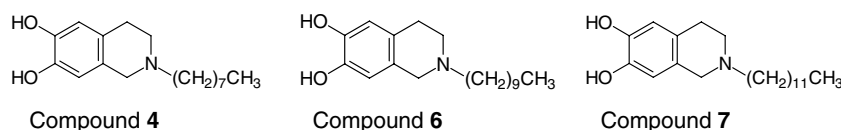


Figure 2.

phobic S3 subsite. The 6,7-phenolic hydroxyl groups were introduced to form H bonds with the residue in the S4 subsite. The tetrahydroisoquinoline ring was selected to act as the skeleton to link the functional groups in the S2 and S3 subsites, and also because of the synthetic accessibility. After energy minimization, the lowest energy position in the active site for the generated lead molecule was determined by the flexible ligand docking procedure in the Affinity module of the Insight II program and scored by the score-3 function in LUDI module. The calculated interaction energies and LUDI scores of each molecule are given in Table 1.

The mode of action of lead molecules **6** with the active site of CYP51 of *C. albicans* is shown in Figure 3. After flexible ligand docking and subsequent molecular dynamics simulated annealing studies, the 6,7-phenolic hydroxyl groups of lead molecule **6** form H bonds with the residue Tyr69, Ser378, Val509 of S4 subsite. At position 2 of the lead structure, long lipophilic alkyl side chains were interacted with the hydrophobic S3 subsite. The tetrahydroisoquinoline ring of lead molecule **6** was interacted with the hydrophobic S2 subsite. No interactions were found between the lead molecule and the heme.

The lead molecules and several of their derivatives were synthesized (Scheme 1): 2-(3,4-dimethoxyphenyl)ethylamine(I) was submitted to Pictet–Spengler reaction using HCHO in acidic ethanol to yield 6,7-dimethoxy-1,2,3,4-tetrahydroisoquinoline hydrochloride (II)²¹ which was neutralized with aqueous NaOH to provide free base(III).²³ The 6,7-dimethoxy-1,2,3,4-tetrahydroquino-

line (III) was refluxed with different alkyl halides to form the intermediates (IV). Cleavage of the methoxy group of IV in HBr/CH₃COOH provided target compounds (V).²⁴

In vitro antifungal activity was measured by means of the minimal inhibitory concentrations (MIC) using the serial dilution method in 96-well microtest plates. Test fungal strains were obtained from the ATCC or were clinical isolates. The MIC determination was performed according to the national committee for clinical laboratory standards (NCCLS) recommendations with RPMI 1640 (Sigma) buffered with 0.165 M Mops (Sigma) as the test medium. The MIC value was defined as the lowest concentration of test compounds that resulted in a culture with turbidity less than or equal to 80% inhibition when compared with the growth of the control. Test compounds were dissolved in DMSO serially diluted in growth medium. The yeasts were incubated at 35 °C and the dermatophytes at 28 °C. Growth MIC was determined at 24 h for *Candida* species, at 72 h for *Cryptococcus neoformans*, and at 7 days for filamentous fungi. In vitro antifungal activity of the lead compounds was shown in Table 1.

The results of in vitro antifungal activities of the novel compounds showed that all of the lead molecules exhibited potent antifungal activities against six pathogenic fungi, and compounds **6**, **7**, exhibited equal or stronger antifungal activities against five test fungi than that of control drug fluconazole except *C. albicans*. The antifungal activities of compounds **1**, **2**, **3**, **4**, **5**, and **9** were lower than those of compounds **6**, **7**, and **8**, suggesting

Table 1. The calculated interaction energies and LUDI scores of the lead molecules

Compound	E_{vdw}	E_{Elec}	E_{Total}^a	Score
4	−44.9629	−11.62	−56.5829	422
6	−45.9949	−15.5208	−61.5157	460
7	−49.7315	−15.1056	−64.8372	606

Calculated interaction energies (kcal/mol) for the complexes of the lead compounds with the active site of CYP51 of *Candida albicans* and Ludi scores.

$$^a E_{\text{Total}} = E_{\text{vdw}} + E_{\text{elec}}$$

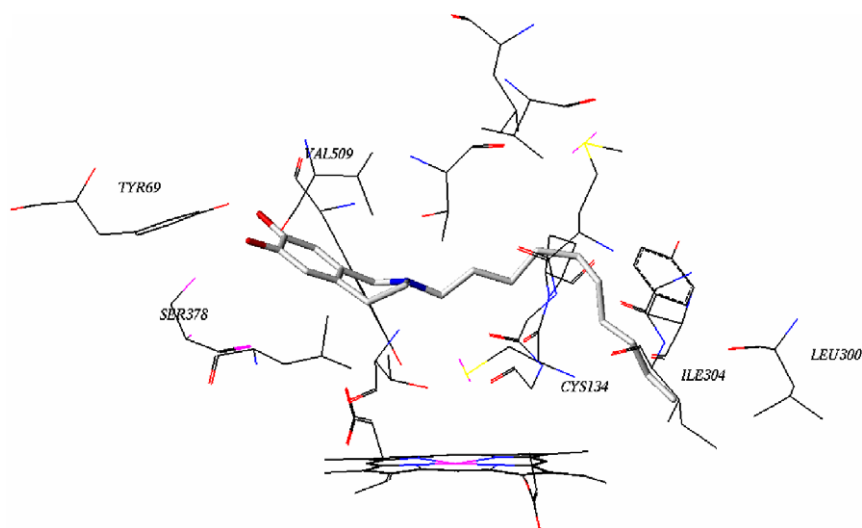
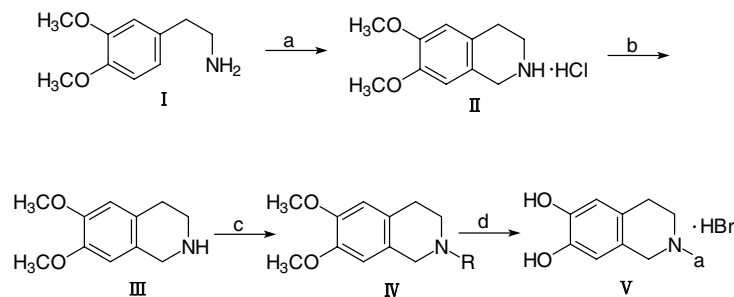


Figure 3. The mode of action of lead molecules **6** with the active site of CYP51 of *Candida albicans*.

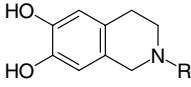


Scheme 1. Reagents and conditions: (a) HCHO/HCl/CH₃CH₂OH, yield 68.7%; (b) NaOH, yield 96.8%; (c) alkyl halides/NaCO₃/CH₃CH₂OH, reflux, yield 71.3–90.5%; (d) HBr–CH₃COOH, reflux, yield 85.3–93.2%.

that the appropriate substitution at position 2 of the compound was important for antifungal activities. Compound **9** was less potent because the alkyl side chain at its position 2 was too long to be accommodated by the hydrophobic S3 subsite. Compounds **1**, **2**, **3**, **4**, and **5** were less potent because their alkyl side chain was too

short to interact firmly with the hydrophobic region, although it was able to enter the active site. The overall trend for the interaction energy and LUDI scores was in good qualitative agreement with the antifungal activities in vitro. All of the results gave us the suggestion to further design and synthesize their derivatives (Table 2).

Table 2. In vitro antifungal activity of the lead compounds

		MIC ₈₀ (ug/ml)					
Compound	R	C. alb.	C. par.	C. neo.	A. fum.	M. can.	T. rub.
1	–(CH ₂) ₄ CH ₃	>200	100	100	>200	>200	>200
2	–(CH ₂) ₅ CH ₃	>200	100	100	>200	>200	>200
3	–(CH ₂) ₆ CH ₃	>200	100	100	>200	>200	>200
4	–(CH ₂) ₇ CH ₃	>200	100	100	>200	50	50
5	–(CH ₂) ₈ CH ₃	200	25	25	200	50	12.5
6	–(CH ₂) ₉ CH ₃	100	12.5	3.125	50	12.5	3.125
7	–(CH ₂) ₁₁ CH ₃	50	50	6.25	50	12.5	12.5
8	–(CH ₂) ₁₃ CH ₃	50	50	6.25	>200	12.5	25
9	–(CH ₂) ₁₅ CH ₃	>200	100	100	200	>200	200
10	Fluconazole	1.562	50	6.25	>200	100	25

Abbreviations: C. alb., *Candida albicans*; C. par., *Candida parapsilosis*; C. neo., *Cryptococcus neoformans*; A. fum., *Aspergillus fumigatus*; T. rub., *Trichophyton rubrum*; M. can., *Microsporium canis*.

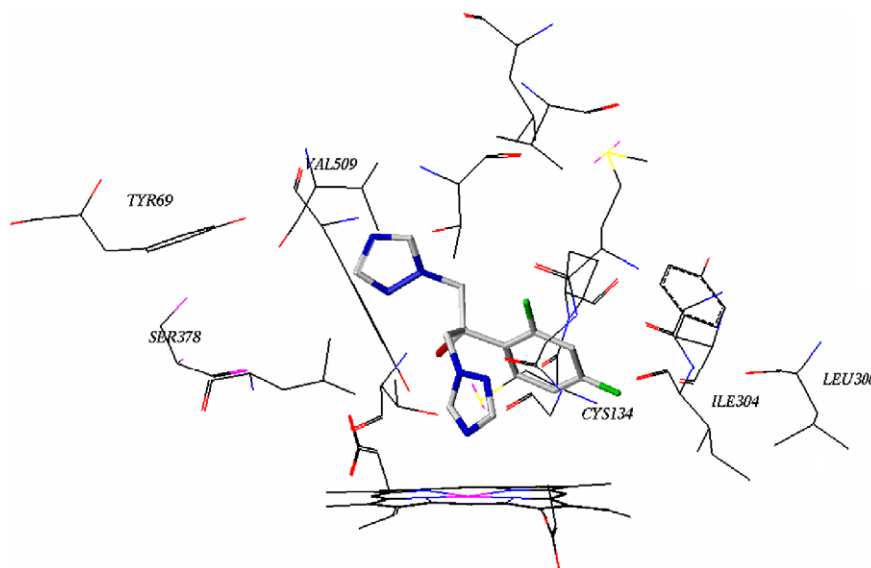


Figure 4. The mode of action of fluconazole with the active site of CYP51 of *Candida albicans*.

In summary, the novel tetrahydroisoquinolines based on lanosterol 14 α -demethylase of fungi were discovered by coupling structure-based de novo design with chemical synthesis, and their antifungal activities in vitro were evaluated. The mode of action of the lead molecules was represented, which was different from that of azoles (Fig. 4). The lead compounds exhibited potent antifungal activities in vitro. Because the affinity of the lead molecules for CYP51 was mainly attributed to their non-bonding interaction with the apoprotein, the studies presented here afford the opportunity to develop novel antifungal agents that specifically interact with the residues in the active site and avoid the serious toxicity arising from coordination binding with the heme of mammalian P450s.

Acknowledgment

The work was supported by the National Natural Science Foundation of China (Grant No. 30572257).

References and notes

- Vanden Bossche, H.; Koymans, L. *Mycoses* **1998**, *41*, 32.
- (a) Kale, P.; Johnson, L. B. *Drug Today (Barc)* **2005**, *41*, 91; (b) Sheehan, D. J.; Hitchcock, C. A.; Sibley, C. M. *Clin. Microbiol. Rev.* **1999**, *12*, 40.
- Georgopapadakou, N. H.; Walsh, T. J. *Antimicrob. Agents Chemother.* **1996**, *40*, 279.
- Lupetti, A.; Danesi, R.; Campa, M.; Tacca, M. D.; Kelly, S. *Trends Mol. Med.* **2002**, *8*, 76.
- Slama, J. T.; Hancock, J. L.; Rho, T.; Sambucetti, L.; Bachmann, K. A. *Biochem. Pharmacol.* **1998**, *55*, 1881.
- Wulff, H.; Miller, M. J.; Hansel, W.; Grissmer, S.; Cahalan, M. D.; Chandy, K. G. *Proc. Natl. Acad. Sci. U.S.A.* **2000**, *97*, 8151.
- Legra, S. A.; Bergemer-Fouquet, A. M.; Jonville-Bera, A. P. *Am. J. Med.* **2002**, *113*, 352.
- Bok, R. A.; Small, E. J. *Drug Safety* **1999**, *20*, 451.
- Su, F. W.; Perumalswami, P.; Grammer, L. C. *Allergy* **2003**, *58*, 1215.
- (a) Wolf, R.; Wolf, D.; Kuperman, S. J. *Clin. Gastroenterol.* **2001**, *33*, 418; (b) Jeng, M. R.; Feusner, J. *Pediatr. Hematol. Oncol.* **2001**, *18*, 137.
- Kauffman, C. A.; Hedderwick, S. A. *Drugs Aging* **2001**, *18*, 313.
- Linnebur, S. A.; Parnes, B. L. *Ann. Pharmacother.* **2004**, *38*, 612.
- Plempel, M. *Shinkin to shinkinsho* **1982**, *23*, 17.
- Fromtling, R. A. *Clin. Microbiol. Rev.* **1988**, *1*, 187.
- Ji, H.; Zhang, W.; Zhou, Y.; Zhang, M.; Zhu, J.; Song, Y.; Lu, J.; Zhu, J. *J. Med. Chem.* **2000**, *43*, 2493.
- Ji, H.; Zhang, W.; Zhang, M.; Kudo, M.; Aoyama, Y.; Yoshida, Y.; Sheng, C.; Song, Y.; Yang, S.; Zhou, Y.; Lu, J.; Zhu, J. *J. Med. Chem.* **2003**, *46*, 474.
- Joseph-McCarthy, D.; Tsang, S. K.; Filman, D. J.; Hogle, J. M.; Karplus, M. *J. Am. Chem. Soc.* **2001**, *123*, 12758.
- Luty, B. A.; Wasserman, Z. R.; Stouten, P. F. W.; Hodge, C. N.; Zacharias, M.; McCammon, J. A. *J. Comput. Chem.* **1995**, *16*, 454.
- Bohm, H.-J. *J. Comput.-Aided Mol. Des.* **1994**, *8*, 243.
- Bohm, H.-J. *J. Comput.-Aided Mol. Des.* **1998**, *12*, 309.
- Mp 252–253 °C (lit.²² 251–252 °C); ¹HNMR (DMSO, 300 MHz): 3.04 (t, 2H, *J* = 6.2 Hz), 3.49 (t, 2H, *J* = 6.3 Hz), 3.81 (s, 3H), 3.82 (s, 3H), 4.28 (s, 2H), 6.81 (s, 1H), 6.87 (s, 1H).
- Bobbitt, J. M.; Kiely, J. M.; Khanna, K. L.; Ebermann, R. *J. Org. Chem.* **1965**, *30*, 2247.
- Mp 82–84 °C (lit.²² 84–85 °C).
- Compound 4·HBr, ¹HNMR (DMSO, 500 MHz): 0.85 (t, *J* = 6.7 Hz, 3H), 1.27–1.79 (m, 12H), 2.95–2.98 (m, 2H), 3.23 (m, 2H), 3.29–3.35 (t, 2H), 4.11–4.4 (dd, *J*_A = 133 Hz, *J*_B = 15.1 Hz, 2H), 6.68 (s, 1H), 6.75 (s, 1H), 9.61 (s, 1H); compound 6·HBr (DMSO, 300 MHz) 0.86 (t, *J* = 6.7 Hz, 3H), 1.26 (m, 14H), 1.73 (s, 2H), 2.73–2.83 (m, 2H), 2.96–3.58 (m, 4H), 4.02–4.33 (dd, *J*_A = 75.2 Hz, *J*_B = 13.6 Hz, 2H), 6.55 (d, *J* = 9.4 Hz, 2H), 9.05 (d, *J* = 13.2 Hz, 2H), 10.05 (s, 1H); compound 7·HBr (DMSO, 500 MHz) 0.86 (t, *J* = 6.8 Hz, 3H), 1.25–1.73 (m, 20H), 2.80 (m, 2H), 2.96 (m, 2H), 3.15–3.65 (m, 2H), 4.09–4.36 (dd, *J*_A = 117.8 Hz, *J*_B = 14.6 Hz, 2H), 6.57 (d, *J* = 13.6 Hz, 2H), 9.04 (d, *J* = 16.5 Hz, 2H), 9.78 (s, 1H).